Assessment of the Engine Installation Performance of a Redesigned Tilt-rotor Intake System

G. A. Misté[1], T. Nibale[2], A. Garavello[3], E. Benini[4]

[1] PhD Candidate, University of Padova, Padova, Italy, gianluigialberto.miste@studenti.unipd.it

[2] Research Engineer, HIT09 Srl, Padova, Italy, t.nibale@hit09.com

[3] Research Engineer, HIT09 Srl, Padova, Italy, a.garavello@hit09.com

[4] Associate Professor, University of Padova, HIT09 Srl, Padova, Italy, ernesto.benini@unipd.it

ABSTRACT

The always growing interest that rotorcraft manufacturers on reducing the environmental impact of their products pushes toward the development of specific methodologies devoted to propulsive efficiency optimization and evaluation of gas turbine engine performance. In particular, the determination of benefits that re-design and optimization of airframe engine installation components have on fuel consumption assume a relevant position in the design process. Optimized inlet and exhaust geometries can be obtained by coupling CFD codes with advanced optimization algorithms, automatically searching for optimal solutions among a prescribed search space. The consortium constituted by the University of Padova (UNIPD) and the spin-off company HIT09 successfully applied this automatic optimization approach to several components of the European tilt rotor ERICA, including engine installation. In this paper, the assessment of the engine performance gain given by such optimization is done using an engine off design performance prediction software, TSHAFT. First, a brief presentation of the code, developed at UNIPD, is given, along with validations carried out on a specific test case found in literature, for which experimental data are known. Subsequently, TSHAFT is employed in the ERICA case, taking into account inlet flow distortion effects. An exhaustive performance comparison between baseline and optimized engine installations is provided, highlighting the remarkable improvement in engine efficiency and compressor stability achieved by means of the optimization method implemented.

INTRODUCTION

Industrial aviation is always more pointing towards new solutions able to reduce noise, air pollution, fuel consumption, and increasing aircraft vehicles overall efficiency. In the general research aimed to the attainment of these specific goals, Clean Sky (see www.cleansky.eu for more elucidations), namely a European Joint Technology Initiative (JTI), represents one of the largest European research project ever launched. Its mission is to develop breakthrough technologies in order to reduce the environmental impact of airplanes and air transport. The JTI consists of 6 integrated technology demonstrators (ITD) that will provide the development of in-flight and ground demonstrators. Among those projects the Green Rotorcraft stands out for its contribute for improving helicopters and tilt-rotor aircrafts. In turn, within Green Rotorcraft ITD, 6 technological proposals have been set

Presented at the American Helicopter Society 68th Annual Forum, Fort Worth, Texas, May 1-3, 2012.

up. Among these, the project Green-Rotor-Craft 2 (GRC-2) is aimed at the reduction of several rotorcraft components drag, so as to increase airframe and non-rotating systems efficiency.

Within the GRC-2, specific sub-tasks are dedicated to the drag reduction assessment of several ERICA (**E**nhanced **R**otorcraft **I**nnovative **C**oncept **A**chievement, [1]) tilt-rotor fuselage components (program CODETilt [2]) and the minimization of engine/airframe integration loss characterizing a tilt-rotor nacelle (program TILTOp [3]), again considering the ERICA as test case. In the framework of those two research programs, the two main investigators, namely the University of Padova (UNIPD) and the spin-off company HIT09, developed a general purpose aerodynamic optimization environment, coupling the in-house UNIPD genetic algorithm GDEA [4] and the commercial CFD analysis tools available at helicopter industries. Then, the so implemented design methodology has been applied to the ERICA components pointed for optimization by the GRC-2 requirements.

The present paper is dedicated to the description of a specific methodology devoted to the performance assessment of turboshaft/turboprop engines and the determination of engine installation efficiency for tilt-rotor configurations; the methodology main purpose is the evaluation of benefits achieved by the ERICA airframe re-design and optimization activities carried out within the GRC-2, from the engine standpoint.

The method is based on the engine simulation code TSHAFT, developed at UNIPD, which is used to determine turboshaft/turboprop on and off design performance in various operational conditions, evaluating the results obtained by inlet and exhaust shape optimization: its implementation includes specific features devoted to the evaluation of inlet flow loss and distortion effect on the engine behavior, so that the impact of different and re-designed intake and/or exhaust system can be effectively quantified.

The paper is structured as follows: firstly, some introductory theoretical definitions and considerations regarding intake performance are exposed. Subsequently, the TSHAFT code is described in all its features and its modeling capabilities are validated against both experimental data and other commercially available software. Finally, the performance assessment of the optimized ERICA engine intake ([5], [6]) is carried out from the engine standpoint using TSHAFT, highlighting the remarkable improvements achieved in terms of both fuel consumption and stability with respect to the compressor surge margin.

In appendix, a brief description of the UNIPD-HIT09 automatic design procedure and its application to the ERICA air intake system is provided. The reader can find the complete discussion on those aspects in [6], which is included in the 68th AHS forum proceeding.

INTAKE PERFORMANCE: THEORETICAL CONSIDERATIONS

Definition of Intake Performance Parameters

The most common measure of intake efficiency is the intake total pressure ratio (pressure recovery); The total pressure ratio represents the efficiency of the intake compression process which transforms the free-stream kinetic energy into static pressure:

$$r = \frac{P_{AIP}}{P_{\infty}} \qquad \textbf{Eq. 1}$$

where P_{AIP} is the total pressure measured at the AIP and P_{∞} is the free stream total pressure.

Both the total pressure ratio and total pressure loss can be evaluated from CFD simulations by means of standard post processing functions.

The air diffusion process, occurring in the intake system, must be accomplished with the minimum loss in total pressure and with the best attainable flow distribution at the intake exit plane. The intake optimization strategy pursued, among others, this goal.

Inlet flow distortion (IFD) affects not only components' efficiency (and thus the thermodynamic cycle), but also penalizes engine performance due to the actions of the control system.

In particular, since aircraft gas turbine engines operate downstream an air intake system, the level of distortion at the compressor face affects the performance and the stability of the compressor itself. If the compressor stall margin is lowered under a certain acceptability level, the control system acts on

mechanical devices to change the position of the engine operating point, and this action typically decreases overall engine performance.

For tilt-rotor inlet applications, the dominant distortion effect is due to total pressure distortion. Total temperature and entropy distortions act in parallel with the total pressure one, except when hot gases from external sources are ingested (i.e. exhaust gases from other aircrafts). Flow angle and swirl distortion affect the compressor behavior in parallel with total pressure distortion, with similar effects; it has been demonstrated that, especially at low incidence flight conditions, total pressure and swirl coefficient have the same trend (an increase of swirl leads to an increase of total pressure distortion [7]).

In order to quantify the flow distortion magnitude, from which both quality of intake flow and engine tolerance can be assessed, the subsequent usual form is utilized:

$$DC(\theta) = \frac{P_{AIP} - P_{\theta}}{q_{AIP}} \qquad \textbf{Eq. 2}$$

where q_{AIP} is the corresponding AIP mean dynamic head and P_θ is the weighted area average total pressure in the "worst" sector of angular extent θ at the engine face, as illustrated in Figure 1. The sector θ must be of significant extent and 60 deg is usually regarded as a satisfactory minimum. Thus a commonly used coefficient is DC(60), adopted for the scope described in this paper.

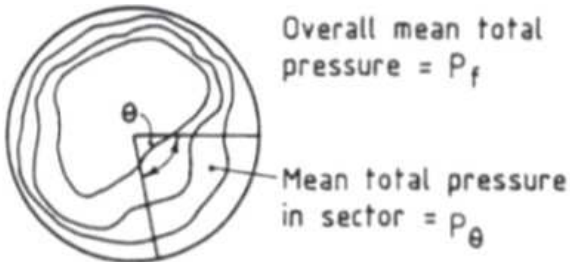

Figure 1: Illustration of total-pressure contours and θ=60deg sector for definition of distortion coefficient [7].

The definition given in Eq. 2 leads to the following simplifying assumption: the upcoming inflow can be ideally divided in two sectors, one supposed to be clean and the other one characterized by a concentrate distortion. Once accepted this modeling assumption, it is useful to calculate the two different recovery factors r_θ and $r_{360°-\theta}$ related respectively to the clean and the spoiled sector. To do this, it is possible to define the DC(θ) as follows [7]:

$$DC(\theta) = \frac{\Delta P_{\theta} - \Delta P_{AIP}}{q_{AIP}} \qquad \textbf{Eq. 3}$$

where ΔP_{AIP} and ΔP_θ are the differences in mean total pressure with respect to the free stream values. Manipulating, it is possible to obtain:

$$DC(\theta) = \frac{P_{AIP}}{q_{AIP}} \frac{P_{\infty}}{P_{AIP}} \frac{(\Delta P_{\theta} - \Delta P_{AIP})}{P_{\infty}} =$$

$$= \frac{P_{AIP}}{q_{AIP}} \frac{1}{r} \left[\frac{\Delta P_{\theta}}{P_{\infty}} - (1 - r) \right] = \qquad \textbf{Eq. 4}$$

$$= \frac{P_{AIP}}{q_{AIP}} \frac{1}{r} [(1 - r_{\theta}) - (1 - r)]$$

from which, since r and DC(θ) are known, the recovery factor in the distorted sector r_θ is derived. To calculate $r_{360°-\theta}$ the following equations are employed:

$$P_{AIP} = P_{\theta} \frac{\theta}{360°} + P_{360°-\theta} \left(1 - \frac{\theta}{360°} \right) \qquad \textbf{Eq. 5}$$

$$r_{360°-\theta} = \frac{P_{360°-\theta}}{P_{\infty}} \qquad \textbf{Eq. 6}$$

From Eq. 5 it is possible to derive $P_{360°-\theta}$ (i.e. the mean total pressure in the clean sector) by which the clean sector recovery factor $r_{360°-\theta}$ can be finally calculated.

Parallel Compressor Theory

The parallel compressor theory (from Kurzke [8]) supposes that IFD can be modeled by two separate flows, one for the clean sector and one for the spoiled sector, so that the flow can be schematized as if it was entering into two parallel compressors. This yields two different operating points on the compressor map, related to the flow properties of the two sectors. These

points are situated on the same corrected speed line for the first compressor, if no temperature distortion is present (as represented in Figure 2); the same would not hold true for the eventual following compressors, since the total temperature value at the compressor exit would be different between the clean and the distorted sector.

According to the parallel compressor theory, even if the undistorted flow operating point is well below the surge line, the compressor is predicted to surge if the operative point of the distorted sector override the surge line, even if the average operating point (M in Figure 2, [8]) has still a positive surge margin. It must be said that, even if the operating point of the spoiled sector is slightly below the surge line, transient phenomena may affect engine behavior, involving compressor instability and surging problems; intake geometry must be designed to avoid this randomness in all flight conditions.

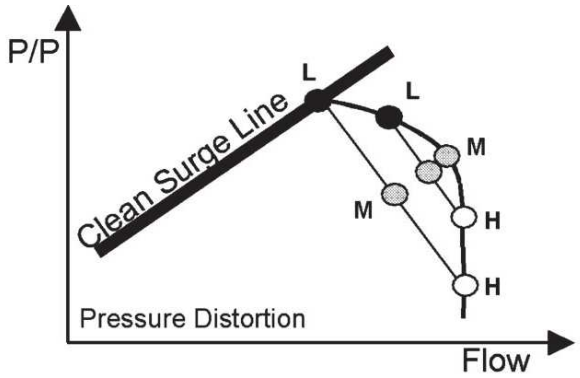

Figure 2: IFD operating points on the same corrected speed line: L represents the distorted sector, H the clean sector and M is the average operating point (courtesy of Kurzke [8]).

To calculate the flow properties in both sectors within an engine deck a new constraint in the matching algorithm must be inserted. This condition, as first approximation, can be given by setting the equality between the values of total pressure related to the clean and distorted flow exiting the first compressor. This is a good approximation when the flow downstream the first compressor is almost uniform, but it is not when the distortion persists inside the following components. A typical case is given by multi-spool axial compressors, in which the inter-duct length does not permit the mixing of the two flows, so that the total pressure uniformity condition leads to inaccurate results. Indeed, this condition tends to overestimate the loss in surge margin of the first compressor, and does not predict stall of the subsequent compressors, which is possible to occur. The opposite condition to total pressure uniformity at the first compressor outlet is given by no mass flow between the two sectors, i.e. complete separation between the clean and distorted sectors, just as if they were separated by an ideal wall. However, some mixing between the flows is a physical evidence. For this reason it is useful to introduce a coupling factor [8], variable between zero (no coupling between compressors, i.e. pressure balance) and unity (full coupling, i.e. no flow between sectors), used to define a new matching constraint, accounting for the two ideal above mentioned conditions. In this way an intermediate condition (decided by the user) between total pressure balance and no flow from one sector to the other, can be simulated, increasing the model accuracy.

TSHAFT ENGINE SIMULATION CODE: BRIEF DESCRIPTION OF THE MODEL

To simulate the engine performance, TSHAFT, an in-house lumped parameters performance prediction software, implemented at the University of Padova, was utilized. The code, written in MatLab® language, has been validated through several comparisons with engine performance data given by experimental measures and commercially available software.

In TSHAFT, the turboshaft engine is modeled by connecting the following components (see Figure 3):

- Inlet
- Compressor
- Combustor
- Gas generator turbine (GGT)
- Free power turbine (FPT)
- Nozzle
- External load.

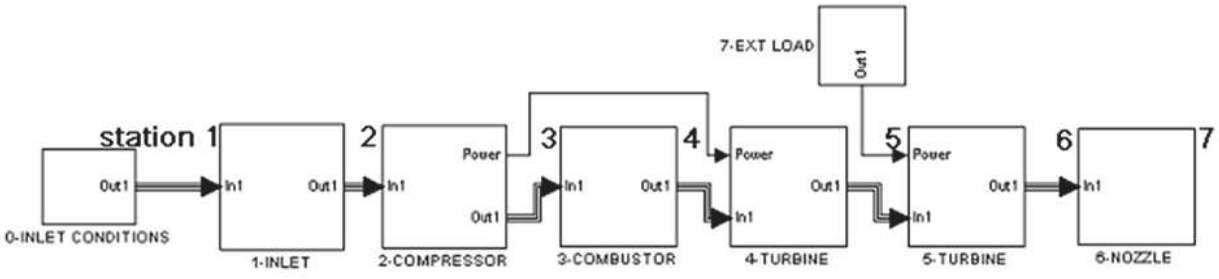

Figure 3: GE T700 engine simplified model implemented in gas turbine simulation code TSHAFT.

The general physical assumptions for the engine model are the following:

1. Steady state operation;
2. Lumped parameters model: within each component there are only input and output values of state variables which do not vary continuously in space;
3. Working fluid consisting of a mixture of ideal gases with variable specific heats;
4. Adiabatic components: each component has no heat exchange with the environment;
5. Thermodynamic irreversibilities are included in calculations through the use of different types of efficiencies.
   Ambient conditions are determined by altitude selection; an ISA standard model is implemented to relate altitude to the values of static pressure and temperature.
6. To account for specific heat variations with temperature, the Shomate equation is used:

$$c_p = A + Bt + Ct^2 + Dt^3 + Et^{-2} \qquad \textbf{Eq. 7}$$

where the temperature coefficient values for each specie composing the operative fluid are provided by NIST tables [9].

Off-Design Steady State Performance Calculations

In a turboshaft engine, several causes determine performance deviation from design conditions [10], such as: (i) variation of ambient conditions; (ii) variation of fluid composition (humidity); (iii) variation of flight Mach number; (iv) variation of mechanical power required by an external load (in our case, the tilt rotor propeller); (v) variation of the engine rotational speed. In TSHAFT, simulations can be performed including the effects of all those variations, taking into account efficiency variations of every single engine component.

Off-design performance is calculated employing different scaled characteristic maps for the various engine components.

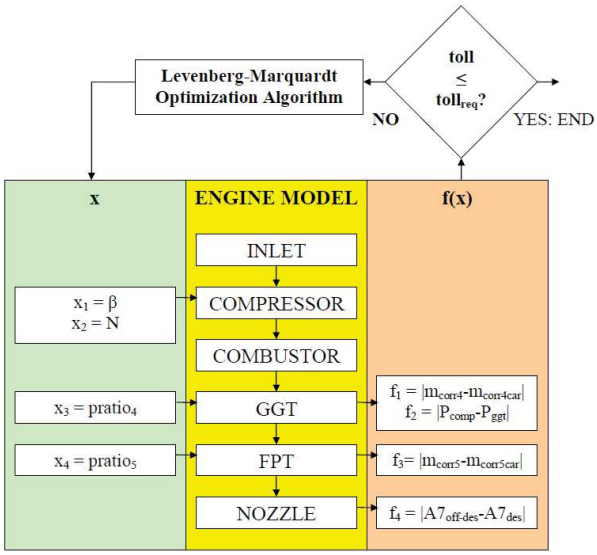

Figure 4: Matrix method used by the Off Design solver for the turboshaft engine of Figure 3.

A matrix method is used to solve for the non-linear equations system resulting from formalization of the matching problem (see also Walsh and Fletcher [11]). In the matching problem, the values of corrected mass flow and power predicted by the thermodynamic model are compared with those obtained through characteristic map interpolation using an iterative Levenberg-Marquardt optimization algorithm [12] (as shown in Figure 4). This methodology guarantees the mass and energy conservation for steady state operations.

Once all the relationships between state variables and performance parameters are defined, a system of the type $f(x) = 0$ is solved, where f is a vector-valued error function (matching constraints) and x is the vector of the variables (matching guesses).

For a detailed description on the thermodynamic model implemented by the TSHAFT simulation code, see [13].

TSHAFT CODE VALIDATION

A single test case of a well-known turboshaft engine with comparisons between experimental data and numerical predictions will be briefly exposed. The tested engine is the GE T700, for which several data are available in literature ([14], [15], [16]). The outputs from the TSHAFT code are compared against the results obtained using the NLR's gas turbine simulation software GSP [17] and against experimental data collected at the NASA Lewis research center. Six different operating conditions are simulated, with different external loads; test specifications are well summarized in ref. [15].

The validation assessment is represented in Figures 5-10. Fuel consumption is probably the most interesting parameter to analyze. The operational points generated by TSHAFT are in good agreement with the experimental data, with a maximum relative error on the various performance quantities in line with and sometimes even better than GSP calculations. The principal cause of discrepancies between experimental and simulations' results might be found mainly in the lack of knowledge of single engine component performance, not only in the accuracy of the two models. However, these comparisons show that the TSHAFT code is a valuable instrument to predict the performance parameters of a generic turboshaft engine. Once confirmed the validity of the code, it will be further demonstrated how this software can be used to calculate the performance variation due to engine installation effects.

ERICA ENGINE SIMULATION

Optimization of the ERICA Air Intake

S-shaped air intakes, such as those mounted at the wing tips of the ERICA tilt rotor, induce a strong secondary flow pattern [18] that causes localized increase or decrease of the relative flow angle value at the first stage compressor blades [19]; moreover, the resulting distorted total pressure and total temperature distribution at the compressor aerodynamic interface plane strongly affects engine performance [20], [21] and can also produce rotating stall instability of the compressor rotor [22]; because of the aforementioned reasons, inlet flow loss and distortion must be accurately calculated and their effects on every engine component must be taken into account.

Nowadays CFD methods provide an effective methodology to evaluate the aerodynamic behavior of a turbo-prop inlet; indeed, numerical simulations allow to accurately predict flow development within an intake duct and to determine the main inlet performance parameters such as total pressure loss and flow distortion. When used as a design tool, CFD allows the evaluation and comparison of performance relative to different inlet designs. Therefore, optimized inlet and exhaust geometries can be obtained by coupling CFD codes with advanced optimization algorithms, automatically searching for optimal solutions among a prescribed search space [5], [6].

Preliminary CFD computations carried out on the ERICA intake baseline configuration highlighted the need to reduce total pressure loss and inlet flow distortion level. In order to achieve this objective, the GDEA based automatic design procedure has been applied [5], [6]. More detailed information about the intake geometry optimization methodology is provided in Appendix.

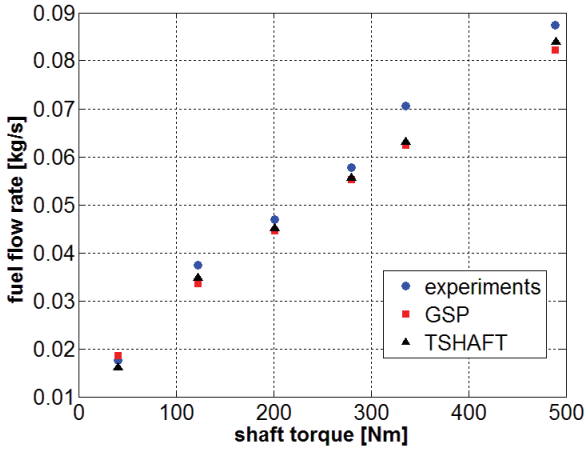

Figure 5: Fuel flow.

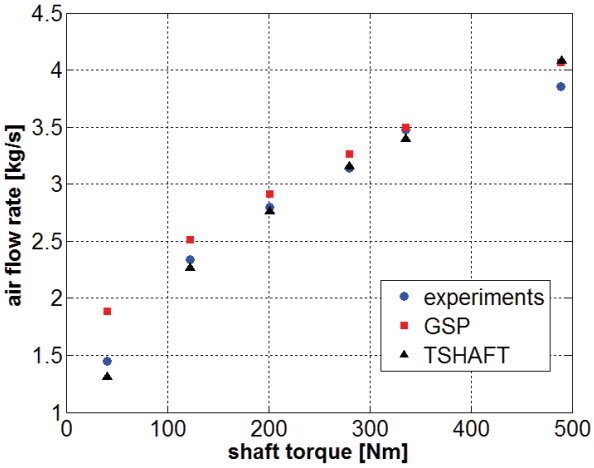

Figure 6: Air mass flow rate.

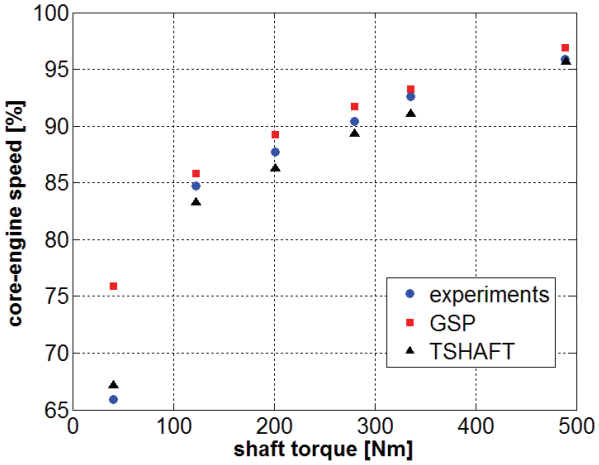

Figure 7: Core-engine speed.

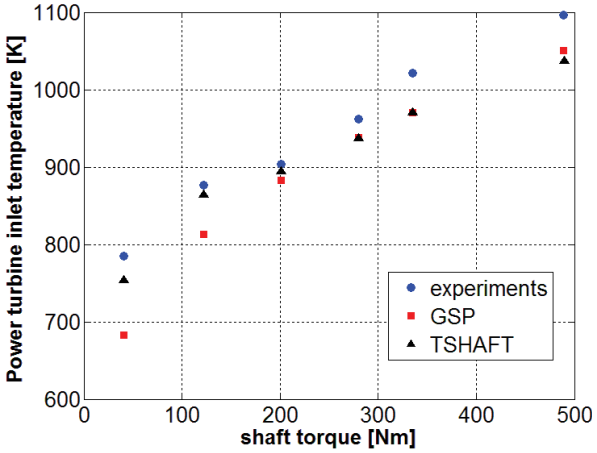

Figure 8: Power turbine inlet temperature.

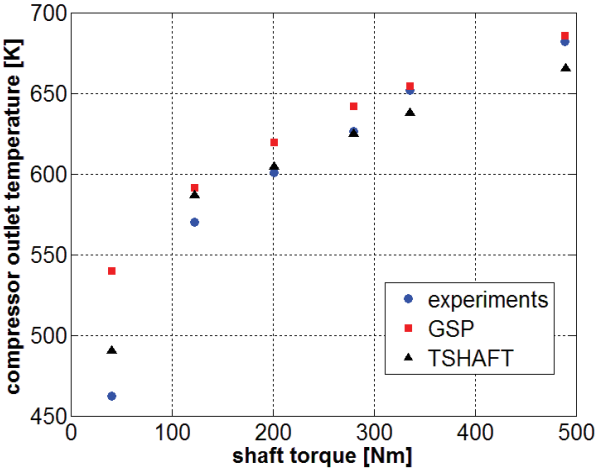

Figure 9: Compressor outlet temperature.

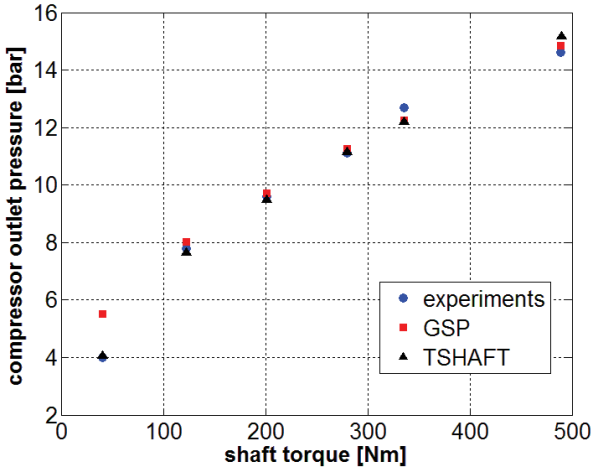

Figure 10: Compressor outlet pressure.

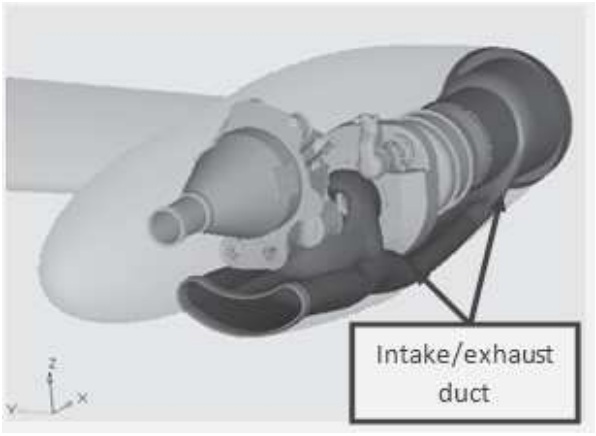

Figure 11: Layout of the ERICA nacelle internal components. Courtesy of GRC2 Consortium.

As can be seen in Figure 11, the ERICA intake system is a single-scoop inlet, being the intake entry located on the lower part of the aircraft nacelle. The rotor spinner approach surface is physically separated from the inlet by means of a boundary layer diverter, which allows avoiding the ingestion of the approach surface perturbed boundary layer through the inlet [7],[18]. The single-scoop solution forces the implementation of an S-shaped duct to connect the entry area and the "*aerodynamic interface plane*" (AIP), which represents the aerodynamic interconnection between the engine face and the intake duct.

Details about the baseline geometrical characteristics and the parameters defined in order to parametrically describe the intake duct geometry within HyperMorph® [23] are reported in [5].

ERICA Engine Simulations and Results

Once the CFD numerical simulations on the ERICA nacelle configuration have been carried out by means of Ansys Fluent® [24], allowing to define the flow characteristics in several relevant flight conditions for both baseline and optimized intake geometry, TSHAFT has then been used to simulate the engine performance in off-design conditions. Being the actual ERICA engine data not available for the authors, the turboprop engine selected for the ERICA simulation is a rescaled GE T700 model, properly modified in order to comply with the level of performance required by the new tilt-rotor concept in its flight envelope.

The simulated engine consists in a low pressure axial compressor (LPC) followed by a high pressure centrifugal compressor (HPC), driven by two corresponding gas turbines, while a free power turbine releases torque to the propeller.

Starting from a common ideal engine design point, in which no intake total pressure losses and no IFD has been taken into account (in accordance with flight data provided by the GRC2 consortium), the effects due to both the intake/exhaust shape optimization and IFD were analyzed in order to realistically determine the compressor stall condition and the overall performance loss estimation.

Predictions of distorted flow and clean flow are considered in two different sectors for the LP axial compressor by TSHAFT, using an integrated parallel compressor model: total pressure distortion is quantified with coefficients which relate spoiled sector values to those in the clean sector. The total pressure loss in the intake component, given as an input to TSHAFT, is computed with the value of r_{duct} derived from the CFD simulations, while the remaining information used to define completely the distorted flow is derived from knowledge of DC(60) and the AIP dynamic head q_{AIP}, also given by the CFD simulations.

The particular configuration of the simulated engine suggests the utilization of a null coupling factor. The reason for this choice is given by the presence of a centrifugal compressor downstream the first axial compressor, for which the parallel compressor theory does not yield accurate prediction results. In addition, the flow inside a centrifugal compressor is much more mixed than in an axial compressor, and thus the pressure balance condition at its inlet appears a reasonable approximation.

To completely determine the engine installation assessment three particular flight conditions are analyzed:

- Cruise - Forward flight (at 7500 m)
- Hover (at sea level)
- Conversion (at sea level)

In a brief information about the rotorcraft flight asset in these three conditions is given; the values of the nacelle setting angles with respect to the free stream direction are listed, along with the intake reverse flow ratio. The nacelle setting angle is defined as the angle between the rotor spinner axis and the fuselage water-line, positive spinner up.

Table 1: Flight conditions, considered for the ERICA intake-engine assessment.

Flight condition	Nacelle setting angle [deg]	Intake inverse flow ratio $\mu = {V_\infty}/{V_{AIP}}$
Cruise	0	1.4
Conversion	60	0.8
Hover	85	0.0

For each condition two off-design steady state simulation sets were carried out, in order to calculate performance parameters and LPC compressor surge margin for both baseline and optimized intake geometry. The level of power required by ERICA to operate at each of the three different flight conditions here analyzed, is chosen as driver for simulations, with the aim to collect data on geometry performance suitable for comparison in each case.

Two models are utilized to compute the performance calculations:

1. **Single flow model**: no IFD are simulated, intake losses are quantified only with the duct pressure recovery factor r;
2. **Parallel compressor model**: two separate flows, one clean and the other spoiled are considered in order to quantify the impact of IFD on performance.

Simulation results are summarized in Figure 12, in which a comparison is made between SFC reduction obtained with the two flow models described above; in abscissa the normalized external load is defined as the shaft torque in each condition divided by the shaft torque value relative to the cruise condition. The same numerical output is also reported in Table 2.

Table 2: Specific fuel consumption for the three flight conditions analyzed.

Flight condition	SFC reduction [%]	
	Single Flow Model	Parallel Compressor Model
Cruise	1.24%	1.54%
Conversion	0.06%	0.12%
Hover	0.08%	0.09%

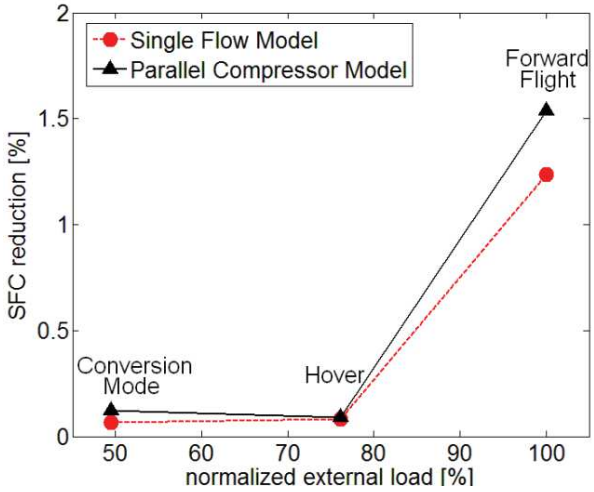

Figure 12: Percentage SFC reduction vs. normalized external load calculated with the Single Flow Model and the Parallel Compressor Model.

In all the three flight conditions considered (and for both the flow models) there has been a SFC reduction deriving from the intake geometry optimization. This result was expected, since the intake total pressure loss in every flight attitude was found to be lower for the new geometry. As it can be seen in Figure 12, the SFC reduction is almost negligible for conversion and hover condition, but is particularly relevant for the cruise condition, in which the aircraft spends most of its flight time. A second observation, regards the comparison between the Single Flow Model and the Parallel Compressor Model: For the hover and conversion cases, the error encountered using the Single Flow Model is very slight. For the cruise condition, however, the SFC reduction expected is 0.3% less than that calculated with the Parallel Compressor Model; this means that the optimized geometry, decreasing the flow distortion level, affects also performance, although not in an extreme way. Therefore, even if this performance difference is useful to be assessed, the true estimation advantages given by the Parallel Compressor Model rely mainly in the possibility to predict and compare the stall margin of the first compressor. Indeed, this task cannot be accomplished with the Single Flow Model.

Figure 18 graphically reports the operating points for both the clean and distorted sectors in all the three flight conditions considered. For the hover and conversion conditions there is no major improvement in surge margin deriving from the intake optimized geometry. However, for the forward flight condition, a much wider surge margin is observed; the baseline geometry distorted operating point is found to be in dangerous proximity of the surge line, whereas the optimized one still maintains an adequate

distance from stall. It must be remarked that the loss in stall margin requires the engine control system to move the engine operating line away from the surge line. This implies the use of inlet guide vanes or blow-off valves, which directly affect engine behavior penalizing overall performance and hence fuel consumption.

CONCLUDING REMARKS

The optimization loop applied to the intake geometry led to a significant decrease in total pressure loss. This implied a direct effect on turboprop engine SFC reduction, especially in cruise flight condition. In addition, the new intake shape allows to reduce the inlet flow distortion magnitude, thus increasing compressor stall margin. This indirectly affects also overall engine performance, as explained in the previous sections. The methodology adopted in the present paper allowed to predict the effect of a shape optimization on the turboprop engine performance. The procedure here exposed may be adopted in the preliminary design phase of new components involving engine assessment, evaluating the worthiness in terms of overall engine performance gain.

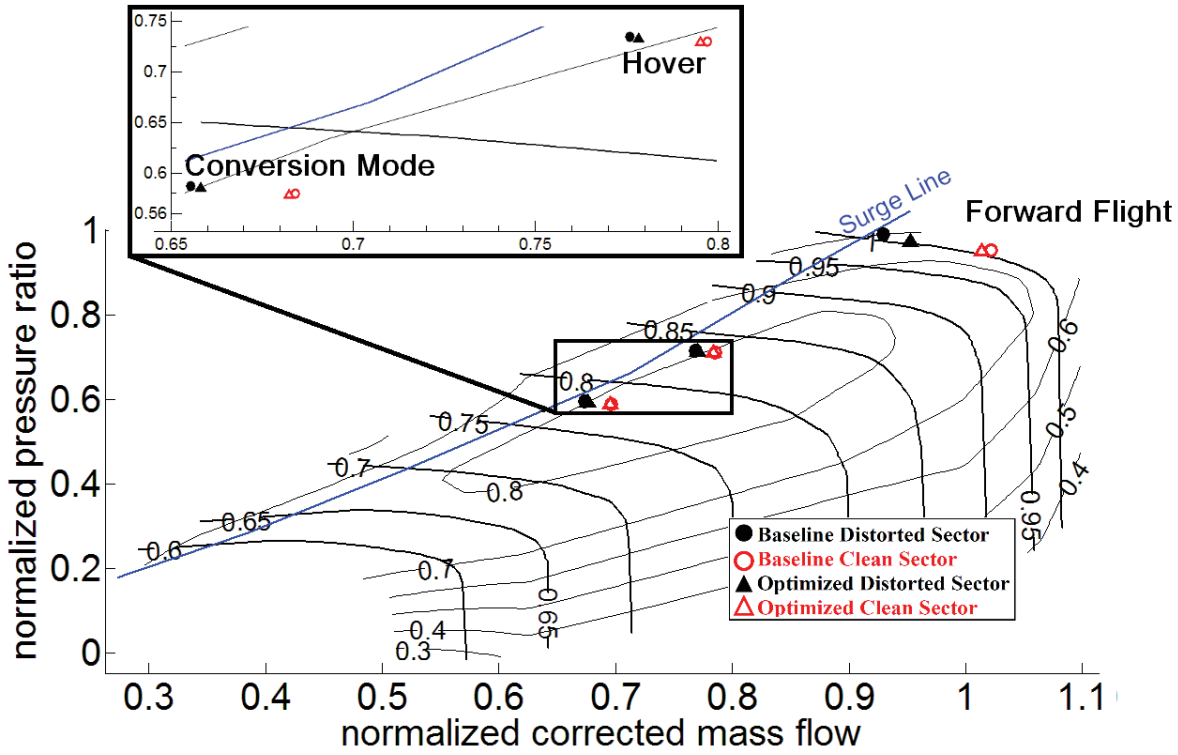

Figure 13: LP Compressor characteristic map with operating points for the three cases considered, calculated with the Parallel Compressor Model: comparison between baseline and optimized intake geometries. Normalization is carried out with respect to the cruise condition.

APPENDIX: DESCRIPTION OF THE INTAKE OPTIMIZATION METHODOLOGY

The aerodynamic optimization procedure applied for the solution of the ERICA intake optimization problem is described in this section.

The automatic chain constituting the automatic optimization block (Figure 14) is built by properly interfacing the three following codes:

1) *GDEA* (Genetic Diversity Evolutionary Algorithm): it is an advanced multi-objective optimization algorithm developed at the University of Padova [4]. It is the selected optimization engine;

2) *Altair HyperMorph*®: it allows the conversion of design parameters selected by GDEA into CFD cases, using mesh morphing algorithms [23], suitable for the objective function evaluation;

3) *Ansys Fluent*®: the selected flow solver [24]; it takes in input the morphed CFD cases coming from

HyperMorph® and gives back to GDEA the correspondent values of the chosen objective functions.

During the optimization process, GDEA let a population of individuals (each one corresponding to a different set of design variables and so to a different geometry configuration) "evolve" until the convergence to the *Pareto optimal frontier* [25] has been reached, being the Pareto frontier the set of non-inferior solutions, which represents the solution of a multi-objective optimization problem. The intrinsic multi-objective approach adopted allows the designer to select, among the Pareto optimal set, the solution which is more suitable for his/her needs without introducing his/her arbitrariness in the problem set up, as commonly happens using traditional optimization approaches. A more exhaustive description of the optimization method is reported in [6].

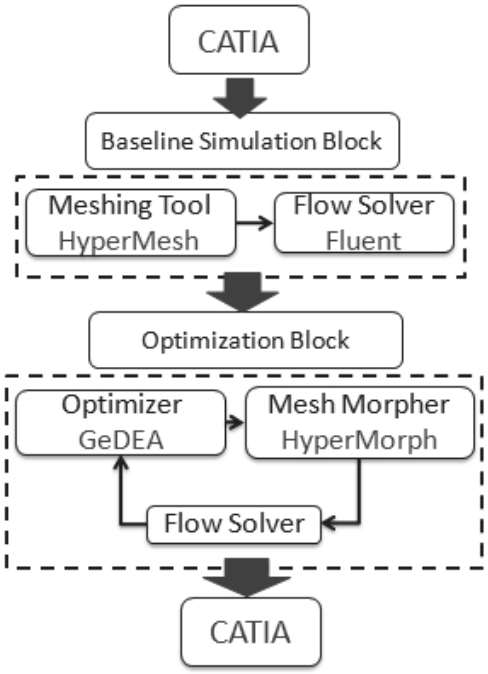

Figure 14: Optimization method flow-chart.

Set up of the Inlet Duct Optimization Problem

The GDEA optimization problem formulation is expressed as follows:

$$Maximize[r, -DC(60)] \qquad \textbf{Eq. 8}$$

The CFD model used for the aerodynamic objective function evaluation, is characterized by an unstructured triangular surface mesh and tetra volume mesh with prismatic layers wall elements. An appropriate disc actuator model with non-uniform pressure jump and rotor induced swirl has been included to take into account the steady state rotor effects. k-ω SST ([26], [27]) turbulence model was chosen as the most accurate.

The flight condition considered during the automatic design phase is high speed, high altitude cruise condition. Then several other flight conditions were considered in order to test the optimized solutions throughout the aircraft flight envelop. For the purpose of this paper, two additional flight conditions are considered, namely an hover condition and a conversion condition. Conversion permits to reach the aircraft horizontal forward flight after a vertical or short track take-off and is characterized by a particular incidence angle and Mach.

Summary of Engine Intake Optimization Results

The intake optimization results are discussed within this section; even if the optimization procedure has been run only for a small number of generations, remarkable improvements can be observed on both the objective functions considered.

Figure 15 shows the Pareto frontier calculated by the GDEA algorithm after ten generations. Maximum total pressure loss reduction amounts to -70% of the baseline value. This particular solution features also a -27% reduction for the distortion index DC(60). Moving on the other side of the Pareto front, the solution featuring the most uniform AIP total pressure distribution is characterized by a DC(60) 44% lower than the baseline value. An interesting compromise between the two objective is the one highlighted in Figure 15, featuring 52% loss reduction and DC(60) 38% lower than baseline.

A detailed optimization results discussion, including comparison between the different intake geometries, is reported in both [5] and [6].

In the proceeding of this paper, the solution highlighted as compromise in Figure 15 is considered for further discussion. Indeed, this particular inlet configuration is characterized by enhanced performance throughout the whole flight envelope of the tilt rotor. Total pressure loss and DC(60) comparisons between baseline and optimized inlets, for the flight conditions enumerated in Table 1, are reported in Figure 16 and Figure 17.

As expected, the most remarkable benefits have been achieved for cruise (52% loss reduction and DC(60) 38% lower than baseline), which was the flight point considered during optimization.

However, the new design is characterized by significant improvements also for conversion (7% reduction of total pressure loss and 9% DC(60) reduction) and hover (6% reduction of total pressure loss and 4% DC(60) reduction).

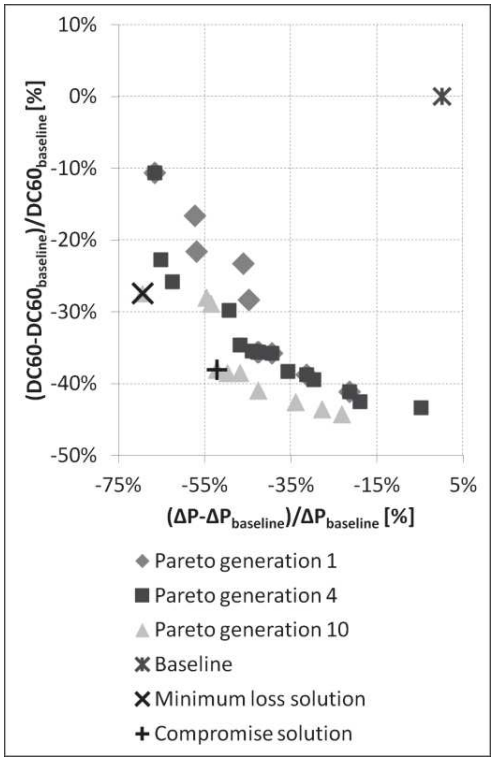

Figure 15: Intake Pareto front after 10 GDEA generations. Evolution through generations and baseline values are also represented [6].

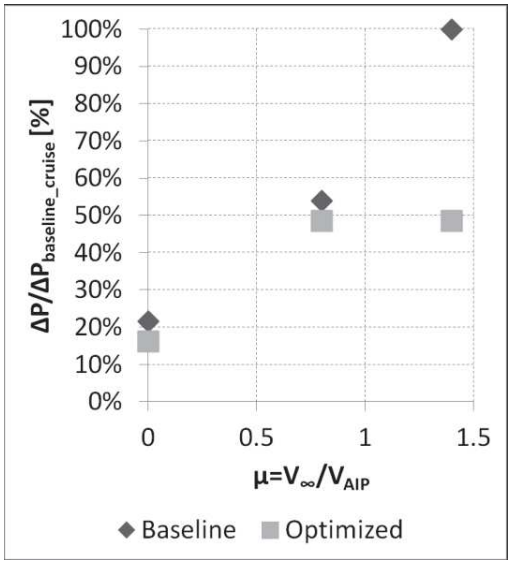

Figure 16: Total pressure loss comparison between the baseline and optimized intake, considering cruise, conversion and hover flight conditions.

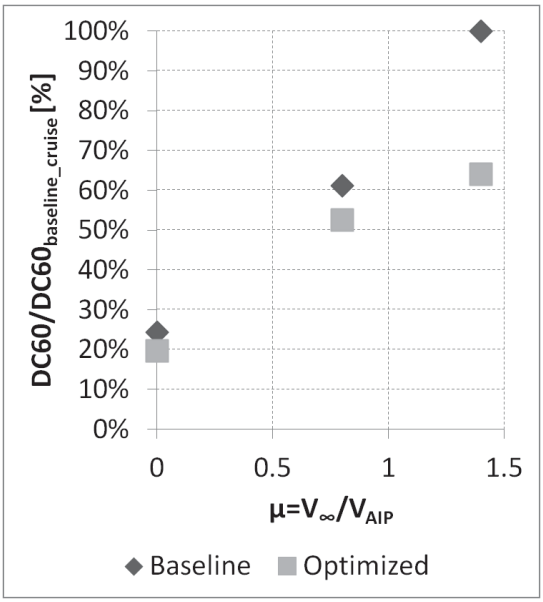

Figure 17: DC60 comparison between the baseline and optimized intake, considering cruise, conversion and hover flight conditions.

REFERENCES

[1] **Nannoni F., Giancamilli G., Cicalè M.**, "Erica: the European advance tilt-rotor", *27th European Rotorcraft Forum*, Moscow, Russia, 11th – 14th September 2001.

[2] **CleanSky JTI call for proposal** JTI-CS-2010-1-GRC-02-004, *Contribution to design optimization of tiltrotor for drag reduction (fuselage/wing junction, nose and landing gear sponsons, empennage)*, available on http://www.cleansky.eu/content/homepage/calls, SP1-JTI-CS-2010-01, pag. 57.

[3] **CleanSky JTI call for proposal** JTI-CS-2009-2-GRC-02-001, *Contribution to the study of the air intake and exhaust integration into a tiltrotor nacelle*, available on http://www.cleansky.eu/content/homepage/calls, SP1-JTI-CS-2009-02, pag. 34.

[4] **Benini E., Toffolo A.**, "Genetic diversity as an objective in multi-objective evolutionary algorithms", *Evolutionary Computation, MIT press journal*, 11(2):151–167, 2003.

[5] **Garavello A., Benini E., Ponza R., Scandoglio A., Saporiti A.**, "Aerodynamic Optimization of the ERICA Tilt-Rotor Intake and Exhaust System", *37th European Rotorcraft Forum*, September 13th-15th, 2011, Ticino Park, Italy Aerodynamic Session, Paper ID 191.

[6] **Garavello A., Benini E., Ponza R.**, "Multi-Objective Aerodynamic Design of Tilt-Rotor Airframe

Components by means of Genetic Algorithms and CFD", *Proceeding of the 68th American Helicopter Society Forum*, May 1th – 13th, 2012, Fort Worth, Texas (USA), Aerodynamic Session.

[7] **Seddon J., Goldsmith L**., *Intake Aerodynamics*, Blackwell Science, 2 edition, 1999.

[8] **Kurzke J.**, "Effects of inlet flow distortion on the performance of aircraft gas turbine", *Journal of Engineering for Gas Turbines and Power*, July 2008.

[9] http://webbook.nist.gov/chemistry (last consultation 18 Feb. 2012).

[10] **Saravanamuttoo H.I.H., Rogers G.F.C., Cohen H**., *Gas Turbine Theory*. Pearson Prentice Hall, 2001.

[11] **Walsh P.P., Fletcher P**., *Gas Turbine Performance*, Blackwell Publishing, 2004.

[12] **Marquardt D**., "An Algorithm for Least Squares Estimation of Nonlinear Parameters", *Journal of the Society for Industrial and Applied Mathematics* Vol. 11, No. 2, 1963, pp. 431-441.

[13] **Misté G. A., Benini E**., "Impact of Turbine Rotational Speed Variability on Performance of a Turboshaft Engine for Helicopter Applications", article submitted to *AIAA Journal of Aircraft*.

[14] **Garavello A., Benini E**., "Preliminary Study on a Wide Speed Range Helicopter Rotor/Turboshaft System", accepted manuscript No. 2011-05-C031526.R2, *AIAA Journal of Aircraft*, 2011.

[15] **Ballin M. G**., "A high fidelity real-time simulation of a small turboshaft engine", *NASA Technical Memorandum 100991*, Ames Research Center, 1988.

[16] **Duyar A., Gu Z., Litt J. S**., "A Simplified Dynamic Model of the T700 Turboshaft Engine", *NASA Technical Memorandum 105805*.1992. available at http://ntrs.nasa.gov/archive/nasa/casi.ntrs.nasa.gov/19920021654_1992021654.pdf (last consultation 18 Feb. 2012).

[17] **Visser, W. P. J., Broomhead M. J**., "GSP, A Generic Object-Oriented Gas Turbine Simulation Environment", *ASME paper 2000-GT-0002*, May 2000 (also available as *Report NLR No. NLR-TP-2000-267* at http://www.nlr.nl/id~4296/lang~en.pdf, last consultation 18 Feb. 2012).

[18] **Seddon J**., "Understanding and countering the swirl in S-ducts: test on the sensitivity of swirl to fences", *Aeronautical Journal*, R.Ae.Soc, 1984

[19] **Guo R. W., Seddon J**., "Some unsteady flow characteristics of two S-shaped intake models tested at high incidence", *Report No. RWG/JS/3/82*, University of Bristol, Departement of aeronautical Engineering, 1982

[20] **Detra R. W**., "The secondary flow in curved pipes", *PhD Thesis*, ETH Zurich, 1953

[21] **Aulehla F., Schmitz D. M**., "Intake swirl and simplified methods for dynamic pressure distortion assessment", *Intake Aerodynamics, VKI Lecture Series*, 1988.

[22] **Farokhi S**., *Aircraft propulsion*, John Wiley & Sons, Inc. 2009.

[23] **Altair Engineering**, *HyperMesh & batchMesher User Guide, 2009.*

[24] **Ansys** Fluent 12.0.16, *User Guide, 2009*.

[25] **Deb K**., *Multi-Objective Optimization Using Evolutionary Algorithms*, Wiley, 2001.

[26] **D.C. Wilcox**, *Turbulence Modeling for CFD*, DCW Industries, Inc., La Canada, California, 1998.

[27] **Menter, F. R**., "Two-Equation Eddy-Viscosity Turbulence Models for Engineering Applications," *AIAA Journal*, Vol. 32, No. 8, August 1994, pp. 1598-1605.